Iranian Journal of Chemical Engineering
Vol. 8, No. 4 (Autumn), 2011, IAChE

CO_x Free Hydrogen Production by Catalytic Decomposition of Methane Over Porous Ni/Al_2O_3 Catalysts

*S. Makvandi, S. M. Alavi**
Reaction Engineering Lab., Chemical Engineering Department,
Iran University of Science and Technology, Tehran - Iran

Abstract

The prepared mesoporous spherical alumina with high-surface area was employed as a support for nickel catalysts in methane decomposition reaction. It was observed that, the catalytic activity of Ni/Al_2O_3 catalysts was high at the initial times of reaction and decreased with time on stream, and finally reached a constant value. The deactivation rate of catalysts is dependent on the catalyst characteristics and the operating conditions. The activity results indicate that, the yield of hydrogen and the structure of deposited carbon are strongly dependent on the loading amount of Ni. The SEM results showed that carbon formed on the catalysts in the form of filamentous carbon. Concerning hydrogen production, the 10%Ni/ Al_2O_3 catalyst leads to a higher yield, due to the higher amount of active phases which can catalyze further the number of methane molecules, while lesser amounts of filamentous carbon were observed on this catalyst than for 5 and 7.5%Ni/ Al_2O_3 catalysts at the same operating condition. The yield of hydrogen and structure of filamentous carbon also significantly depend on the reaction temperatures and residence time of gas in the reactor, as the 10%Ni/ Al_2O_3 catalyst showed a remarkable stability with a decrease of about 14% at 800 °C and 25 ml/min after 240 min of reaction. The obtained results showed that the prepared Ni/ Al_2O_3 catalysts had a good activity in methane decomposition reaction, which is one of the highest activities among those for low nickel loaded catalysts reported up until now.

Keywords: *Methane Decomposition, Ni/Al_2O_3, Carbon Filaments, CO_x-Free Hydrogen*

1. Introduction

Hydrogen is a clean energy and a suitable feeding gas when used as a fuel in fuel cells. Steam reforming, partial oxidation and auto-thermal reforming of methane are the major routes for the production of hydrogen. These existing methods have a significant effect on global warming, since they release CO_x (x=1 or 2), while producing hydrogen due to mixing methane with water and oxygen [1]. Therefore, the co-products of these routes, CO and CO_2, must be removed by subsequent steps. The complete removal of CO_x is not economical; as a result, the H_2 thus produced is not suitable for low-temperature fuel cells given that the catalyst

* Corresponding author: alavi.m@iust.ac.ir

is poisoned by CO_x[2].

So, the development of environmentally friendly methods of producing hydrogen is very helpful from the aspect of preventing global warming and saving energy. An alternative process for hydrogen production to conventional routes is the catalytic decomposition of methane as the main component of natural gas [3-5]:

$$CH_4 \rightarrow C + H_2 \quad (1)$$

Due to the absence of oxygen this endothermic reaction has no side-reactions and the need for additional downstream reactions, such as water-gas shift and selective oxidation, is eliminated. Furthermore, the methane decomposition reaction produces a useful byproduct, the deposited carbon, usually as nanomaterials [6-9]. The size and texture of nanomaterials is a function of both the composition and structure of the catalysts used in the methane conversion process [10]. Nickel-based catalysts have been found to be an effective catalytic component in the decomposition of methane to produce hydrogen and carbon [6-11]. Generally Ni is supported on different carriers, such as Al_2O_3, SiO_2, MgO, and zeolit [11–15] in the methane decomposition reaction because of the simplicity of catalyst preparation and high-scale production.

In this study the mesopore alumina was selected as a support for nickel catalyst in methane decomposition and the effect of nickel loading and the operation condition on hydrogen production and quality of carbon was investigated.

2. Experimental

The Al_2O_3 support was prepared as described by Almeida et al. [11] in detail. In this study, before impregnation, the supports were heated at 550°C for 1 hr at a heating rate of 5 °C/min in order to eliminate the carbon. Supported nickel catalysts were prepared by excess-solution impregnation using Al_2O_3 spheres and an aqueous solution of $Ni(NO_3)_2.6H_2O$ of the appropriate concentration to obtain a 5, 7.5 and 10 wt.% nickel content. After impregnation the spheres were dried overnight at room temperature and calcined at 550 °C for 1 h in air at a heating rate of 5 °C/min [7, 9, 10, 12, and 13].

Characterization of the prepared catalysts was carried out by BET, X-ray diffractometry, Temperature-programmed reduction and scanning electron microscopy. The surface areas (BET) were determined by nitrogen adsorption at -196 °C using an automated gas adsorption analyzer (NOVA 2200 system). The pore size distribution was calculated from the desorption branch of the isotherm by the Barrett, Joyner and Halenda (BJH) method. The XRD patterns were recorded on an X-ray diffractometer (Philips PW-1800) using a Cu-Ka monochromatized radiation (λ = 1.542˚A) in the range 2θ=10–80° and the beam voltage and currents of 40Kv and 30mA, respectively. Phase identifications were carried out by comparing the collected spectra with spectra in the database. Temperature-programmed reduction (TPR–H_2) was performed in an automatic apparatus (Micrometric Pluse-ChemiSorb-2705 TPR, Quantachrome) equipped with a thermal conductivity detector. The fresh catalyst (150 mg) was

submitted to a heat treatment (5 °C/min up to 1000°C) in a gas flow (46 ml/min) of the mixture H_2:Ar (3:50). Prior to the TPR, the samples were out gassed under inert atmosphere, at 300°C for 3 h. Hydrogen consumption was measured by analyzing the effluent by means of a thermal conductivity detector. Scanning electron microscopy (SEM) investigation was performed with Philips- XL30 instrument operated at 30 Kv, fixed in a copper tape, with a layer of gold deposited on it, in a vacuum chamber.

Activity measurements were carried out in a vertical fixed-bed continuous-flow reactor made of an 8 mm i.d. stainless-steel tube operated at atmospheric pressure in a down flow mode, and heated by an electric furnace. The reactor was charged with 50 mg of the prepared catalyst. Prior to the reaction, the catalyst was reduced in situ at 700 °C for 90 min in flowing H_2 (20 ml/min) and the reactor temperature was adjusted to reaction temperatures (700, 750 and 800°C) in a flow of N_2 (30 ml/min).

After that, a reactant gas feed consisting of a mixture of CH_4 and N_2 (CH_4/N_2 = 1/6 vol.%) was introduced into the reactor, and the activity tests were performed at different temperatures, ranging from 700 to 800 °C in steps of 50 °C that were kept for 240 min at each temperature, and the flow of methane was then stopped while the nitrogen continued to flow until the reactor was cooled down to room temperature.

The gas composition of the reactants and products were analyzed using a gas chromatograph equipped with a TCD and a Carbosphere column. No methane decomposition products other than hydrogen were detected in the gas phase using this detection system. The conversion of methane was determined using calibrated data and efficiency of the catalysts was reported in terms of methane conversions. The first analysis was done about 10 min after methane was flowed over the catalyst.

3. Results and discussion

3-1. Structural properties of the catalysts

The pore size distributions and N_2 adsorption/desorption isotherms of the Al_2O_3 catalysts are shown in Fig. 1. The obtained results, shown in Fig. 1 and Table 1, indicate that the addition of nickel to the support led to obtaining a sphere with narrower pore size distribution, smaller average pore diameter and lower surface area, suggesting that the impregnated nickel blocks some pores in the support.

A comparison of the N_2 adsorption/ desorption isotherms of Al_2O_3 and Ni/Al_2O_3 (Fig. 1b) shows no clear difference in their patterns due to nickel addition.

The nitrogen adsorption/desorption isotherms, shown in Fig. 1b can be classified as a type IV isotherm, typical of mesoporous materials. According to IUPAC classification, the hysteresis loop is type H_2, indicating a complex mesoporous structure. This type of hysteresis is characteristic of solids consisting of particles crossed by nearly cylindrical channels or made by aggregates (consolidated) or agglomerates (unconsolidated) of spherical particles [16].

The SEM micrographs of typical Al_2O_3 spheres before and after the heat treatment are displayed in Fig. 2. Micrographs of the untreated support show (Fig2.a and b) that the carbon, as large crystals, lay in the alumina media. Elimination of organic

materials through the thermal treatment is evident from SEM analysis. The SEM images of the heat-treated Al_2O_3 sphere indicate that the formation of mesopores takes place as a result of removal of the organic material. Similar observations were reported during support preparation by R.M. de Almeida et al. [11].

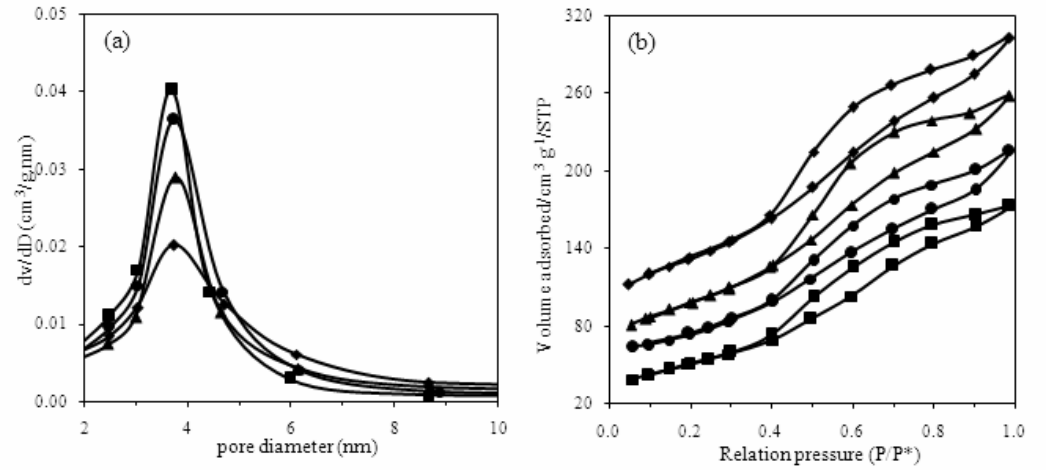

Figure 1. (a) pore size distributions and (b) N_2 desorption/desorption isotherms of the Ni/Al_2O_3 catalysts, ♦ Al_2O_3, ▲ $5\%Ni/Al_2O_3$, ● $7.5\%Ni/Al_2O_3$, ■ $10\%Ni/Al_2O_3$

Table 1. Structural Properties of the Ni/Al_2O_3 catalysts

Sample	Ni loading (%)	BET area (m^2/gr)	Pore volume (cm^3/gr)	Pore diameter (nm)
Al_2O_3	---	280	0.383	6.0457
Ni/Al_2O_3	5	249	0.352	5.6781
Ni/Al_2O_3	7.5	248	0.331	5.1894
Ni/Al_2O_3	10	245	0.303	4.9571

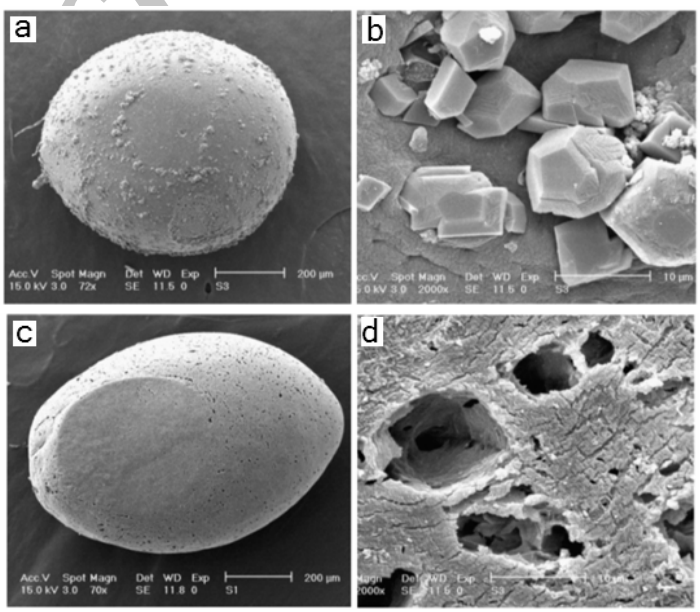

Figure 2. SEM pictures of the spherical Alumina before (a and b) and after (b and c) the heat treatment

Fig. 3 shows the XRD patterns of the calcined catalysts prepared by impregnation of alumina sphere calcined at 550 °C for 1 h. As can be seen, three major peaks are observed at 2θ=36, 45 and 66 that are attributed to the presence of γ-Al_2O_3 phase (JCPDS No. 47-1308). The presence of these peaks indicates that the γ-Al_2O_3 phase has been formed in the applied calcination temperature. The XRD pattern of the catalyst also shows a small peak at $2\theta=60^o$, which can be assigned as either NiO (JCPDS No. 47-1049) or $NiAl_2O_4$ phase (JCPDS card 10-0339). However, because of the weak, broad, and partially overlapping peaks, the crystallite size determination of the Ni-containing phase was difficult. Although it is not easy to identify the difference between the intensities of the Ni-containing phase's peaks, it seems a lower intensity is obtained on the lower nickel loaded catalysts, which means an increase in nickel crystallite size or a decrease in nickel dispersion has been achieved with increasing nickel loading.

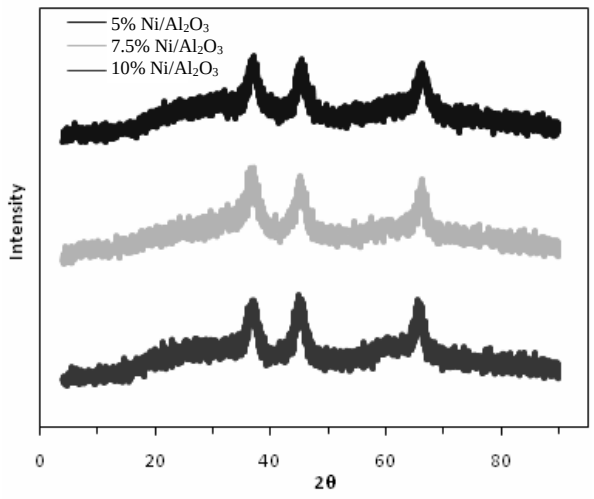

Figure 3. XRD patterns of the calcined catalysts

Fig. 4 presents the results of temperature-programmed reduction (TPR) of the Ni/Al_2O_3 catalysts. The H_2 uptakes were increased with Ni loading, suggesting the bulk property of H_2-TPR. For all the samples two major H_2 consumption steps were observed. The first peak at low temperatures (around 400°C and 500°C) could be due to the reduction of NiO [17], which has a low interaction with the support, and the second peak at higher temperatures (around 600°C), which are related to reduction of $NiAl_2O_4$ [17] with higher interaction with the support. The TPR profiles of the catalysts have the same tendency, but by increasing the amount of Ni, the range of H_2 consumption became narrower, the intensity of the peak located at 400°C increased, and the reduction peak corresponding to $NiAl_2O_4$ was shifted to lower temperatures.

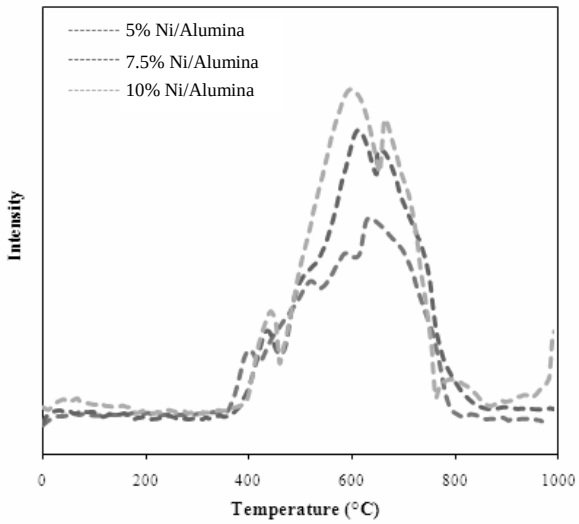

Figure 4. TPR profiles of the catalysts, (a) 5% Ni/Al_2O_3, (b) 7.5% Ni/Al_2O_3 and (c) 10% Ni/Al_2O_3

3-2. Catalytic performance

Fig. 5 shows changes of the methane conversion as a function of time on stream during the catalytic decomposition of methane at 700 °C over Ni/Al_2O_3 catalysts

with different metal loadings. All tests were carried out for 4 hr under identical reaction conditions in order to examine the influence of Ni loadings on alumina. Hydrogen was the only detected product in the effluent gas during the reactions, thus carbon and hydrogen were the only products of this reaction. In Fig. 5 it can be seen that methane conversion value for $5\%Ni/Al_2O_3$ catalyst was high in the beginning of the reaction, then decreased rapidly by time on stream, finally reaching a constant value. The catalyst deactivation is attributed to the deposition of carbon on the surface of the active phase that isolated the active sites and prevented the access of fresh hydrocarbon to the catalyst surface [18].

As can be seen in Fig. 5, an increase in the nickel loading of the catalysts leads to a decrease in the catalyst deactivation rate and a slight increase in the methane conversion value at the end of the reaction. This behavior may be related to the formation of further number of active phase on the surface of the catalysts promoted by the higher nickel loading, which can catalyse a greater number of the methane molecules to carbon and hydrogen. In this sense, the active phase is more accessible in the samples with higher nickel loading; as a consequence, the $10\%Ni/Al_2O_3$ catalyst has the greatest activity during the whole reaction time.

Furthermore, from the results of Fig. 4 it can be seen that with increasing Ni loading, the H_2 uptakes in the TPR profiles were increased and the reduction peak centered in a narrower temperature range, suggesting that the amount of species with lower metal-support interaction was increased. By increases in the concentration of NiO phase, the catalyst becomes more active and the active metal sites are more attainable for the breaking of the C-H bonds in the CH_4 cleavage to produce H_2. This phenomenon may be responsible for the higher CH_4 conversion observed over higher Ni loaded catalyst.

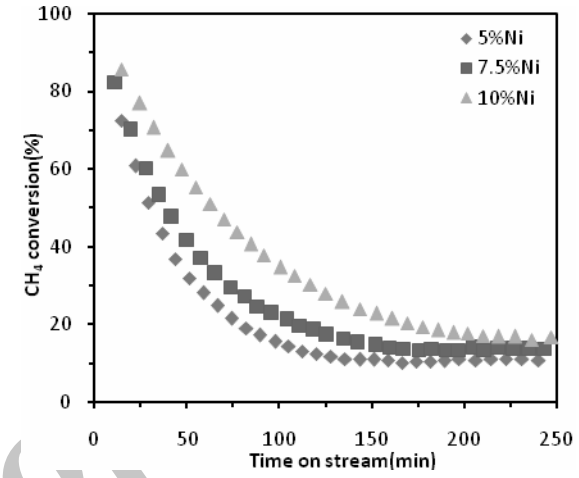

Figure 5. Effect of Ni loading on the performance of the Ni/Al_2O_3 catalysts at 700°C, 35ml/min

The effect of reaction temperature on the methane conversion was investigated over $10\%Ni/Al_2O_3$, which was the most active catalyst for methane decomposition at 700°C, and results are shown in Fig. 6. The temperatures were changed in moderate temperatures from 700 to 800°C in steps of 50°C. It can be seen in Fig. 6 that changes in reaction temperature have a drastic effect on the catalyst activity decaying, as a rapid fall was observed in methane conversion at 700°C, whereas when temperature increased to 800°C, methane conversion occurred with a soft decaying.

An increase in the reaction temperature causes a decrease in the $10\%Ni/Al_2O_3$ catalyst deactivation rate, hence a remarkable increase in the residual value of methane decomposition. This behavior is a

consequence of the fact that, the methane decomposition is a moderately endothermic reaction and increases in the temperature are perfectable in order to increase the equilibrium conversion of methane.

However, increasing in the reaction temperature does not always lead to an increase in catalyst activity [8,12,13,19], because at high temperature reactions the much more rapid initial rate of methane decomposition results in more rapid carbon deposition, which blocks the pores of the catalyst and hinders methane diffusion, leading to the rapid deactivation of the catalyst; but in this study the investigated temperature range was selected in the moderate temperatures that have been studied in previous works [11, 21-23].

The same trend with the 5 and 7.5%Ni/Al_2O_3 also observed similar effects of the reaction temperature on the methane conversion for 10-Ni/Al_2O_3 (results are not shown).

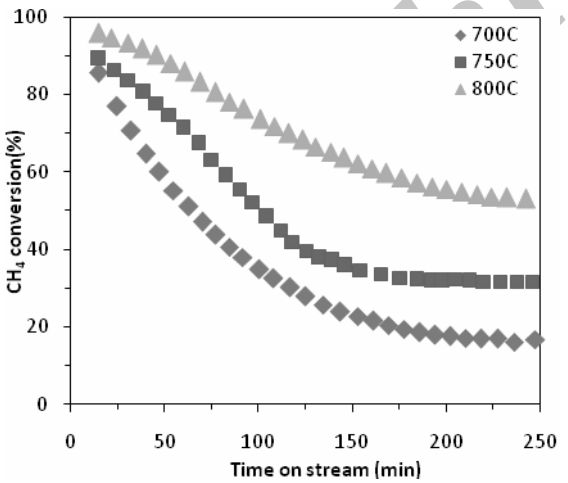

Figure 6. Effect of reaction temperature on the performance of the 10%Ni/Al_2O_3 catalyst at 35ml/min

Fig. 7 shows the methane conversion as a function of time on stream over 10%Ni/Al_2O_3 catalyst, obtained at different gas flow rates and 800 °C. It can be seen that an increase in gas flow rate from 35 to 45ml/min caused a slight decrease in the initial methane conversion, an increase in the deactivation rate, and a remarkable decrease in the residual value of methane conversion. This decrease in methane conversion that was affected by the increasing gas flow rate is a consequence of the methane-catalyst contact time decreases. As the flow rate increases, some of the methane just passes through the voids in the catalyst bed without coming into contact with any active metallic catalyst sites. In catalytic methane decomposition reaction, if a methane molecule does not come into direct contact with an active catalytic site, it will not undergo decomposition. In contrast, with gas flow rate decreasing from 35 to 25ml/min it is observed that catalyst activity just shows a slight decrease, and methane conversion was constant in spite of the increasing amount of carbon deposited. It seems that, this gas flow rate provided enough contact time between methane and active phase, and the rate of methane decomposition was equal to the rate of carbon formation on the surface of the catalyst; consequently, the formation of hydrogen is not hindered by catalyst encapsulation. This fact could explain the high catalyst activity at the end of reaction shown in Fig. 7. The catalyst is most efficient in producing hydrogen at the lowest flow rate and highest reactant-catalyst contact time.

3-3. Sample characterization after catalytic tests

Fig. 8 shows the SEM images used catalysts at 35ml/min for 240 min. On the SEM image

of the 5% Ni/Al_2O_3 sample after reaction at 800°C, filamentous carbon with an average diameter of 40 nm can be observed. The whole catalyst surface was covered by these filaments, which prevent the observation of its morphology. The SEM image of the 7.5%Ni/Al_2O_3 shows that the higher and interlaced filamentous carbons with an average diameter size about 50 nm were formed on the surface of the catalyst. The carbon filaments with relatively thicker diameters were formed over 10%Ni/Al_2O_3 catalyst at 700°C. These results are consistent with formation of greater nickel oxides on the surface of catalysts with higher nickel loading.

As can be seen, the deposited carbon on the 10%Ni/Al_2O_3 catalyst at 800 °C was more amorphous than that of the observed carbon at 700 °C, and the diameter of the filaments was thicker, indicating that the sintering process occurred at a higher temperature.

4. Conclusions

The prepared mesoporous spherical alumina with high-surface area was employed as a support for nickel catalysts in methane decomposition reaction. The deactivation rate of catalysts is dependent on the catalyst characteristics and the operating conditions.

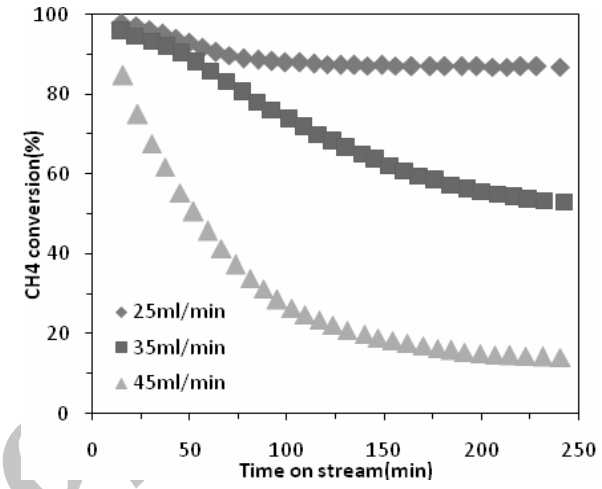

Figure 7. Effect of residence time on the performance of the 10%Ni/Al_2O_3 catalyst at 800 °C

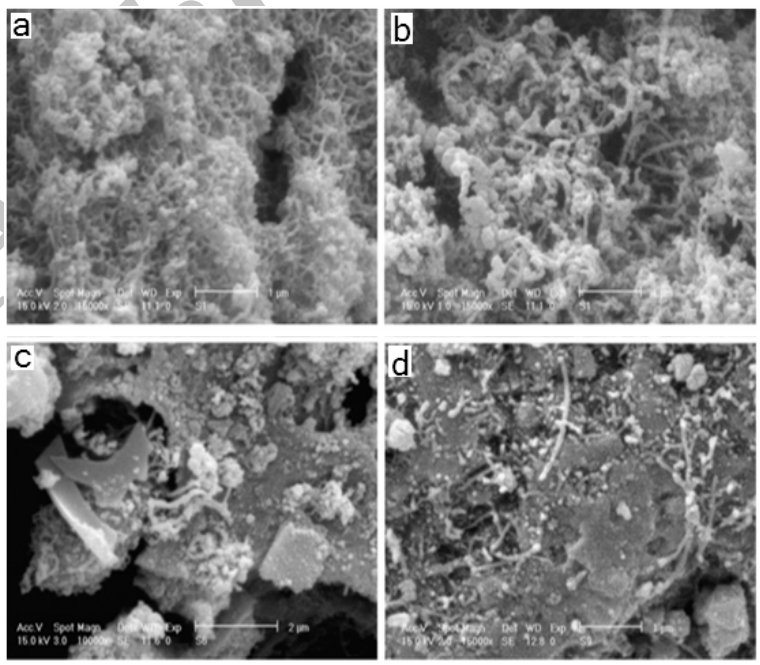

Figure 8. SEM pictures of the spent catalysts after 240 min of reaction, (a) 5% Ni/Al_2O_3 at 800 °C, (b) 7.5% Ni/Al_2O_3 at 800 °C, (c) 10% Ni/Al_2O_3 at 800 °C and (d) 10% Ni/Al_2O_3 at 700 °C.

At a fixed temperature and residence time, an increase in the nickel loading leads to a decrease in the catalyst deactivation rate and a slight increase in the final methane conversion value, especially at the higher temperature. The highest hydrogen yield was obtained by using the 10%Ni/Al_2O_3 catalyst, however, the highest amounts of filamentous carbons were observed on the 7.5%Ni/Al_2O_3 catalyst.

An increase in the reaction temperature causes a decrease in the catalyst deactivation rate, and thus a remarkable increase in the residual value of methane decomposition. An increase in gas flow rate causes a slight a slight decrease in the initial methane conversion, an increase in the deactivation rate, and a remarkable decrease in the residual value of methane conversion. In contrast, with gas flow rate decreasing from 35 to 25ml/min, the catalyst activity just shows a slight decrease and methane conversion maintains a constant value in spite of the increasing amount of carbon deposited.

References

[1] Muradov, N. Z. and Veziroglu, T. N., ""Green" path from fossil-based to hydrogen economy: An overview of carbon-neutral technologies", Int. J. Hydrogen Energy., 33, 6804 (2008).

[2] Choudhary, T.V. and Goodman, D.W., "CO-free fuel processing for fuel cell applications", Catal. Today., 77, 65 (2002).

[3] Muradov, N. Z., "CO_2-Free Production of Hydrogen by Catalytic Pyrolysis of Hydrocarbon Fuel", Energy Fuels, 12, 41 (1998).

[4] Shah, N., Panjala, D. and Huffman, G. P., "Hydrogen Production by Catalytic Decomposition of Methane",Energy Fuels, 15, 1528 (2001).

[5] Ermakova, M. A., Ermakov, D. Yu., Chuvilin, A. L. and Kuvshinov, G. G.," Decomposition of Methane over Iron Catalysts at the Range of Moderate Temperatures: The Influence of Structure of the Catalytic Systems and the Reaction Conditions on the Yield of Carbon and Morphology of Carbon Filaments", J. Catal., 201, 183 (2001).

[6] Noda, L.K., Goncalves, N.S., Valentini, A., Probst, L.F.D. and de Almeida, R.M., "Effect of Ni loading and reaction temperature on the formation of carbon nanotubes from methane catalytic decomposition over Ni/SiO_2", J. Mater. Sci., 42, 914 (2007).

[7] Chai, S., Sharif Zein, S. H. and Mohamed, A. R., "Synthesizing carbon nanotubes and carbon nanofibers over supported-nickel oxide catalysts via catalytic decomposition of methane", Diamond & Related Materials, 16, 1656 (2007).

[8] Bai, Z., Chena, H., Li, B. and Li, W., "Methane decomposition over Ni loaded activated carbon for hydrogen production and the formation of filamentous carbon", Int. J. Hydrogen Energy., 32, 32 (2007).

[9] Piao, L., Li, Y., Chen, J., Chang, L. and Lin, J. Y.S., "Methane decomposition to carbon nanotubes and hydrogen on an alumina supported nickel aerogel catalyst", Catalysis Today, 74, 145 (2002).

[10] Chen, D. E. Christensen, K. O., Fernandez, E. O., Yu, Z., Totdal, B., Latorre, N., Monzón, A. and Holmen, A., "Synthesis of carbon nanofibers: effects of Ni crystal size during methane decomposition",J. Catal., 229, 82 (2005).

[11] De Almeida, R. M., Fajardo, H. V., Mezalira, D. Z., Nuernberg, G.B., Noda, L. K., Probst, L.F.D. and Carreno, N.L.V., "Preparation and evaluation of porous nickel-alumina spheres as catalyst in the production of hydrogen from decomposition of methane", J. Mole. Catal. A: Chemical, 259, 328 (2006).

[12] Villacampa, J.I., Royo, C., Romeo, E., Montoya, J.A., Del Angel, P. and Monzón, A., "Catalytic decomposition of methane over $Ni-Al_2O_3$ coprecipitated catalysts: Reaction and regeneration studies", Applied Catalysis A: General, 252, 363 (2003).

[13] Takenaka, S., Kobayashi, S., Ogihara, H. and Otsuka, K., "Ni/SiO_2 catalyst effective for methane decomposition into hydrogen and carbon nanofiber", J. Catal., 217, 79 (2003).

[14] Bonura, G., Blasi, O. D., Spadaro, L., Arena, F. and Frusteri, F., "A basic assessment of the reactivity of Ni catalysts in the decomposition of methane for the production of "COx-free" hydrogen for fuel cells application", Catalysis Today, 116, 298 (2006).

[15] Ashok, J., Kumar, S. N., Venugopal, A., Kumari, V. D. and Subrahmanyam, M., "CO_X-free H_2 production via catalytic decomposition of CH_4 over Ni supported on zeolite catalysts", Journal of Power Sources, 164, 809 (2007).

[16] Rezaei, M., Alavi, S.M., Sahebdelfar, S., Bai, P., Liu, X. and Zi-Feng Y., "CO_2 reforming of CH_4 over nanocrystalline zirconia-supported nickel catalysts", Applied Catalysis B: Environmental, 77, 346 (2008).

[17] Echegoyen, Y., Suelves, I., Lazaro, M.J., Moliner, R. and Palacios, J.M., " Hydrogen production by thermo-catalytic decomposition of methane over Ni-Al and Ni-Cu-Al catalysts: Effect of calcination temperature ", Journal of Power Sources, 169, 150– (2007).

[18] Kepinski, L., "Inhibiting effect of metal-support reaction on carbonization of $NiSiO_2$ films", Carbon, 30, 949 (1992).

[19] Ermakova, M.A., Ermakov, D.Yu. and Kuvshinov, G.G., "Effective catalysts for direct cracking of methane to produce hydrogen and filamentous carbon: Part I. Nickel catalysts", Applied Catalysis A: General, 201, 61 (2000).

[20] Suelves, I., Lazaro, M.J., Moliner, R., Echegoyen, Y. and J.M. Palacios, "Characterization of NiAl and NiCuAl catalysts prepared by different methods for hydrogen production by thermo catalytic decomposition of methane", Catalysis Today, 116, 271 (2006).

[21] Suelves, I., Lzaro, M.J., Moliner, R., Corbella, B.M. and Palacios, J.M., "Hydrogen production by thermo catalytic decomposition of methane on Ni-based catalysts: influence of operating conditions on catalyst deactivation and carbon charac-teristics", International Journal of Hydrogen Energy, 30, 1555 (2005).

[22] Monzon, A., Latorre, N., Ubieto, T., Royo, C., Romeo, E., Villacampa, J.I., Dussault, L., Dupin, J.C., Guimon, C. and Montioux, M., "Improvement of activity and stability of Ni–Mg–Al catalysts by Cu addition during hydrogen production by catalytic decomposition of methane", Catalysis Today, 116, 264 (2006).